Splitting methods for relaxation two-phase flow models

H. Lund [a,*], P. Aursand [b]

[a]Dept. of Energy and Process Engineering, Norwegian University of Science and Technology (NTNU), NO-7491 Trondheim, Norway

[b]SINTEF Energy Research, Sem Sælands vei 11, NO-7465 Trondheim, Norway

[*]Corresponding author: halvor.lund@ntnu.no

Abstract. *A model for two-phase pipeline flow is presented, with evaporation and condensation modelled using a relaxation source term based on statistical rate theory. The model is solved numerically using a Godunov splitting scheme, making it possible to solve the hyperbolic fluid-mechanic equation system and the relaxation term separately. The hyperbolic equation system is solved using the multi-stage (MUSTA) finite volume scheme. The stiff relaxation term is solved using two approaches: One based on the Backward Euler method, and one using a time-asymptotic scheme. The results from these two methods are presented and compared for a CO_2 pipeline depressurisation case.*

Keywords: hyperbolic conservation laws; relaxation; splitting methods.

1   INTRODUCTION

Two-phase flow is present in many industrial applications, such as heat exchangers, oil and gas production, CO_2 transport and storage, and in the nuclear industry. Modelling of such flows is known to be a challenging task, much due to the possibly complex behaviour of the interface in different flow regimes, and heat and mass transfer across this interface.

If the precise shape of the interface is of little interest or too computationally expensive to calculate, one can apply *averaging* of the physical quantities over a certain area or volume. This typically leads to systems of hyperbolic conservation laws conserving mass, momentum and energy. Transfer of heat, mass and momentum between the two phases can then be modelled in the form of source terms in these conservation equations. In this paper, we will focus on the modelling and numerical solution of a mass transfer term which models evaporation and condensation between the liquid and gas phase. Evaporation of liquid in a pipeline will cause potentially large temperature drops, rendering the pipe steel brittle and vulnerable to rupture, and is therefore crucial to predict.

Source terms for mass may be stiff, i.e. the time scales associated with the relaxation process might be significantly shorter than those of the hyperbolic flux term in the fluid-dynamical model. A stiff source term requires careful numerical treatment to avoid instabilities. One method to accomplish this, is to use a fractional-step (or splitting) method, which divides the problem into two parts: The hyperbolic conservation equations and the source term. These two parts can then be solved separately using methods well suited for each part.

Our paper is organized as follows: In Section 2, we present the models needed to describe the fluid-mechanical behaviour as well as the mass transfer. The numerical methods for solving these models are presented in Section 3, where we describe the splitting procedure, followed by methods for solving the hyperbolic fluid-mechanical equation system and the mass transfer source term separately. We present numerical results for a CO_2 pipeline depressurisation case in Section 4 and compare the results for two different numerical methods. Finally, Section 5 summarizes our work and outlines possible further work.

2 MODELS

To construct a model for two-phase flow with phase transfer, we need a fluid-mechanical model, a model to describe the phase transfer, and a thermo-dynamic model or equation of state (EOS). In the following, we will present each of these models.

2.1 Fluid-mechanical model

Fluid-mechanical models for two-phase flow are often averaged over a certain area or volume to reduce the computational cost and remove the need to explicitly model the location of the gas-liquid interface. Such averaged models are typically formulated as conservation equations for mass, momentum and energy. In order to focus on the effect of the numerical solution of the phase transfer model, we wish to use a fluid-mechanical model which is as simple as possible. We choose a four-equation homogeneous flow model, with one mass balance (continuity) equation for each phase, together with equations for conservation of total momentum and energy,

$$\frac{\partial(\alpha_{\mathrm{g}}\rho_{\mathrm{g}})}{\partial t} + \frac{\partial(\alpha_{\mathrm{g}}\rho_{\mathrm{g}}v)}{\partial x} = \Gamma, \tag{1}$$

$$\frac{\partial(\alpha_{\ell}\rho_{\ell})}{\partial t} + \frac{\partial(\alpha_{\ell}\rho_{\ell}v)}{\partial x} = -\Gamma, \tag{2}$$

$$\frac{\partial(\rho v)}{\partial t} + \frac{\partial(\rho v^2 + p)}{\partial x} = 0, \tag{3}$$

$$\frac{\partial E}{\partial t} + \frac{\partial[(E + p)v]}{\partial x} = 0, \tag{4}$$

where α_k is the volume fraction and ρ_k is the density of phase k, where k is g (gas) or ℓ (liquid). The mixture density is $\rho = \alpha_{\mathrm{g}}\rho_{\mathrm{g}} + \alpha_{\ell}\rho_{\ell}$, and the mixture energy is $E = \alpha_{\mathrm{g}}\rho_{\mathrm{g}}e_{\mathrm{g}} + \alpha_{\ell}\rho_{\ell}e_{\ell} + \frac{1}{2}\rho v^2$, where e_k is the internal energy of phase k. This model has been analysed by e.g. Flåtten et al. [1] in the non-stiff limit $\Gamma = 0$. To close the model, we have assumed that the two phases have equal pressures p, temperatures T and velocities v. The phase transfer appears as a source term, Γ, in the mass balance equations (1)–(2).

2.2 Phase transfer model

Modelling phase transfer between gas and liquid can be done using a variety of different approaches, and there does not seem to exist a universally correct one. Among the most common are kinetic theory, non-equilibrium (irreversible) thermodynamics and statistical rate theory (SRT). The latter is a rather newly suggested approach, based on statistical mechanics. It was first introduced by Ward et al. [2] and later applied to modelling of liquid evaporation [3]. One of the main reasons for the development of SRT was to be able to explain the anomalous temperature profiles found close to an evaporation interface [4].

Lund and Aursand [5] were able to develop an explicit expression for the phase transfer source term Γ in Eqs. (1)–(2) based on SRT. They found an interfacial flux per area expressed as

$$J = \rho_{\mathrm{g}}\sqrt{\frac{k_{\mathrm{B}}T}{2\pi m}}\left(\exp\left[\frac{m(\mu_{\ell} - \mu_{\mathrm{g}})}{k_{\mathrm{B}}T}\right] - \exp\left[\frac{m(\mu_{\mathrm{g}} - \mu_{\ell})}{k_{\mathrm{B}}T}\right]\right), \tag{5}$$

where m is the molecular mass and k_{B} the Boltzmann constant. The chemical potential per mass of phase k is denoted μ_k. This flux has the important property that it reduces to zero when the chemical potentials are equal.

We also need to approximate the interfacial area across which the flux J flows. Since we have an averaged fluid-mechanical model, we have little information about the precise shape of the interface. Hence we make the assumption that the flow is stratified-like, and approximate the interfacial area with [5]

$$A_{\mathrm{int}} = \begin{cases} 4DL(\alpha_{\mathrm{g}} + \delta)\alpha_{\ell} & \text{if } \mu_{\mathrm{g}} < \mu_{\ell}, \\ 4DL\alpha_{\mathrm{g}}(\alpha_{\ell} + \delta) & \text{if } \mu_{\mathrm{g}} \geq \mu_{\ell}, \end{cases} \tag{6}$$

where D the diameter of the pipe and L is the length of the interface in x-direction. The term δ is a tunable *initial volume fraction* which ensures that the evaporation or condensation can start even when the mass-receiving phase

has zero volume fraction. To ensure that this term only has a small effect, it should be kept smaller than typical volume fraction values, so $\delta \ll 1$.

With the given flux (5) and interfacial area (6), we find the following expression for the phase transfer source term in Eqs. (1)–(2) [5]:

$$\Gamma = \begin{cases} \frac{32\rho_{\mathrm{g}}(\alpha_{\mathrm{g}}+\delta)\alpha_\ell}{\pi D}\sqrt{\frac{m}{2\pi k_{\mathrm{B}}T}}(\mu_\ell - \mu_{\mathrm{g}}) & \text{if } \mu_{\mathrm{g}} < \mu_\ell, \\ \frac{32\rho_{\mathrm{g}}\alpha_{\mathrm{g}}(\alpha_\ell+\delta)}{\pi D}\sqrt{\frac{m}{2\pi k_{\mathrm{B}}T}}(\mu_\ell - \mu_{\mathrm{g}}) & \text{if } \mu_\ell \leq \mu_{\mathrm{g}}, \end{cases} \tag{7}$$

where we have expanded the exponentials to first order in $\mu_{\mathrm{g}} - \mu_\ell$. This model has the advantage of having an explicit mathematical expression, as well as being based on well-established physics principles such as statistical mechanics.

2.3 Equation of state

We have chosen to use the stiffened gas equation of state (see e.g. Ref. [6]), which has the advantage of allowing analytical expressions for most thermodynamic relations, while still being sophisticated enough to give reasonable results for a certain range of pressures and temperatures. It can essentially be seen as an ideal gas with a stiffening term, p_∞, which allows a non-zero density at zero pressure, making it suitable to model liquids as well as gases. The pressure, internal energy and chemical potential in a stiffened gas are given by

$$p(\rho, T) = \rho(\gamma - 1)c_v T - p_\infty, \tag{8}$$

$$e(\rho, T) = c_v T + \frac{p_\infty}{\rho} + e_*, \tag{9}$$

$$\mu(\rho, T) = \gamma c_v T + e_* - c_v T \ln\left(\frac{T}{T_0}\left(\frac{\rho_0}{\rho}\right)^{\gamma-1}\right) - s_0 T, \tag{10}$$

where γ is the ratio of specific heats, c_v is the heat capacity at constant volume and e_* is the zero point of energy. The reference temperature, density and entropy are denoted T_0, ρ_0 and s_0, respectively. Each phase has its own set of parameters, which can be fitted to experimental values.

3 NUMERICS

The fluid-mechanical equation system (1)–(4) can be compactly formulated as

$$\frac{\partial \boldsymbol{q}}{\partial t} + \frac{\partial \boldsymbol{f}(\boldsymbol{q})}{\partial x} = \boldsymbol{s}(\boldsymbol{q}), \tag{11}$$

where $\boldsymbol{q} = [\alpha_{\mathrm{g}}\rho_{\mathrm{g}}, \alpha_\ell\rho_\ell, \rho v, E]$, $\boldsymbol{f}(\boldsymbol{q})$ is the flux function and $\boldsymbol{s}(\boldsymbol{q})$ is the source term. There typically exist well-developed methods for solving homogeneous equation systems, i.e. with $\boldsymbol{s} = 0$. However, if the source term is stiff, problems relating to stability may arise. Therefore, we choose to solve Eq. (11) using a first-order fractional-step method known as Godunov splitting [7, Ch. 17]. This advances the solution $\boldsymbol{q}^n$ from time t_n to time $t_{n+1} = t_n + \Delta t$ using two steps:

1. Solve the hyperbolic homogeneous conservation law given by

$$\frac{\partial \boldsymbol{q}}{\partial t} + \frac{\partial \boldsymbol{f}(\boldsymbol{q})}{\partial x} = 0, \qquad t \in [t_n, t_{n+1}], \qquad \boldsymbol{q}(t_n) = \boldsymbol{q}^n, \tag{12}$$

   yielding an intermediate solution $\boldsymbol{q}^*$.

2. Solve the ordinary differential equation given by

$$\frac{\partial \boldsymbol{q}}{\partial t} = \boldsymbol{s}(\boldsymbol{q}), \qquad t \in [0, \Delta t], \qquad \boldsymbol{q}(t = 0) = \boldsymbol{q}^*, \tag{13}$$

   giving the solution at time t_{n+1}.

This method will be first-order accurate in time as long as each of the two steps are at least first-order accurate in time. With such a fractional-step (splitting) scheme, we can employ efficient, accurate and stable numerical methods in each step, constructed specifically for each part of the problem. In the following, we will describe methods for solving Eqs. (12)–(13).

3.1 Hyperbolic conservation law

As fluid-mechanical models typically are formulated as conservation laws, as is the case with Eq. (12), they are often solved using finite volume methods, which ensure that the physically conserved variables are also conserved numerically. By integrating Eq. (12) over a control volume i, we get

$$\frac{\mathrm{d}\boldsymbol{Q}_i}{\mathrm{d}t} = -\frac{1}{\Delta x}(\boldsymbol{F}_{i+1/2} - \boldsymbol{F}_{i-1/2}), \tag{14}$$

where Δx is the control volume size, $\boldsymbol{Q}_i$ is the average of the conserved variable $\boldsymbol{q}$ over control volume i, while $\boldsymbol{F}_{i+1/2}$ is the numerical flux between control volumes i and $i+1$. As expected from a conserving scheme, the quantity $\boldsymbol{Q}_i$ is only changed due to fluxes in and out. The challenge now lies in approximating the fluxes $\{\boldsymbol{F}_{i+1/2}\}$ at the control volume interfaces, knowing only the control volume averages $\{\boldsymbol{Q}_i\}$. This can be visualized as a discontinuity in $\boldsymbol{Q}$ at each interface at time t_n, and solving for later times is known as solving a Riemann problem.

The multi-stage (MUSTA) approach was first proposed by Toro [8], and is based on solving the Riemann problem at each interface by introducing a local grid and local time stepping. This method can be divided into three steps, which are also illustrated in Figure 1.

1. At each cell interface, define a local grid with $2N$ cells

2. Do M time steps in each local grid, using a first-order centred FORCE flux

3. Use the fluxes from the local grids as fluxes in the original grid
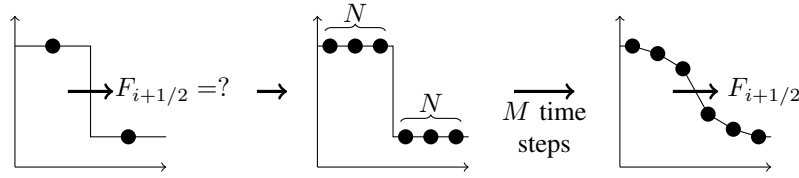

Figure 1: Illustration of the steps in the MUSTA method for *one* interface, between control volumes i and $i+1$.

To calculate the fluxes in the local grid, we use a first-order centred scheme known as FORCE. This flux is given by [9]

$$\boldsymbol{F}_{j+1/2}^{\mathrm{FORCE}} = \frac{1}{2}(\boldsymbol{F}_{j+1/2}^{\mathrm{LF}} + \boldsymbol{F}_{j+1/2}^{\mathrm{Rj}}), \tag{15}$$

where $\boldsymbol{F}_{j+1/2}^{\mathrm{LF}}$ is the Lax-Friedrichs flux

$$\boldsymbol{F}_{j+1/2}^{\mathrm{LF}} = \frac{1}{2}(\boldsymbol{f}(\boldsymbol{Q}_j) + \boldsymbol{f}(\boldsymbol{Q}_{j+1})) - \frac{\Delta x}{2\Delta t}(\boldsymbol{Q}_{j+1} - \boldsymbol{Q}_j), \tag{16}$$

and $\boldsymbol{F}_{j+1/2}^{\mathrm{Ri}}$ is the Richtmyer flux. It is computed by first defining an intermediate state

$$\boldsymbol{Q}_{j+1/2}^{\mathrm{Ri}} = \frac{1}{2}(\boldsymbol{Q}_j + \boldsymbol{Q}_{j+1}) - \frac{\Delta t}{2\Delta x}(\boldsymbol{f}(\boldsymbol{Q}_{j+1}) - \boldsymbol{f}(\boldsymbol{Q}_j)), \tag{17}$$

and then setting the flux to

$$\boldsymbol{F}_{j+1/2}^{\mathrm{Ri}} = \boldsymbol{f}(\boldsymbol{Q}_{j+1/2}^{\mathrm{Ri}}). \tag{18}$$

With the FORCE flux (15), we can then perform time steps on the local grid using a finite volume scheme in a form equivalent to Eq. (14). The time step used in the local grid is calculated using a *local* CFL criterion, given by

$$\Delta t_{\mathrm{loc}} = \frac{C_{\mathrm{loc}}\Delta x}{\max_{1\le j\le 2N}\left(\max_{1\le p\le d}|\lambda_j^p|\right)},$$

where $C_{\mathrm{loc}} \in (0,1)$ is the local CFL number. λ_j^p is the pth eigenvalue of the Jacobian $\partial_{\boldsymbol{q}}\boldsymbol{f}(\boldsymbol{q})$ at grid point i. The denominator is simply the largest (absolute) eigenvalue in the local grid.

Before each time step, we apply extrapolation boundary conditions, $\boldsymbol{Q}_0^m = \boldsymbol{Q}_1^m$ and $\boldsymbol{Q}_{2N+1}^m = \boldsymbol{Q}_{2N}^m$, where the superscript m denotes the mth time step. After the Mth time step, we have found the flux to use in the global grid, namely $\boldsymbol{F}_{N+1/2}^M$. Summarized, the local time steps at each control volume interface are performed as follows [10]:

1. Compute fluxes using Eq. (15).

2. If $m = M$, then return flux $\boldsymbol{F}^M_{N+1/2}$ to be used in global grid.

3. Apply extrapolation boundary conditions: $\boldsymbol{Q}^m_0 = \boldsymbol{Q}^m_1$ and $\boldsymbol{Q}^m_{2N+1} = \boldsymbol{Q}^m_{2N}$.

4. Update solution forward in time using a local finite volume scheme similar to Eq. (14), for $j \in \{1, 2, ..., 2N\}$. Increase m and by one repeat from step 1.

In our numerical simulations presented in Section 4, we will use a MUSTA 2-2 method ($M = N = 2$), with 4 local grid cells and 2 local time steps, similar to the one described by Munkejord et al. [11].

3.2 Relaxation ODE

The second part of the splitting scheme concerns the relaxation term, formulated as the ODE

$$\frac{\partial \boldsymbol{q}}{\partial t} = \boldsymbol{s}(\boldsymbol{q}), \qquad t \in [0, \Delta t], \qquad \boldsymbol{q}(t = 0) = \boldsymbol{q}^*. \tag{19}$$

When the time scales of the relaxation process (19) become significantly smaller than the time scales of the hyperbolic conservation law (12), we are dealing with a stiff relaxation system. For efficiency and simplicity, it is often of interest to resolve the solution at time scales comparable with those of the conservation law. However, doing so in a robust manner requires an ODE solver for (19) with good stability properties. In particular, there is a risk of *overshooting* the equilibrium in the ODE step of the fractional-step method, due to large time steps Δt.

Backward Euler

For first-order accuracy, an obvious choice is the implicit Backward Euler scheme, given by

$$\boldsymbol{q}^{n+1} = \boldsymbol{q}^* + \boldsymbol{s}(\boldsymbol{q}^{n+1}). \tag{20}$$

For monotonic relaxation ODEs such as (19), the Backward Euler scheme is unconditionally stable in the sense that a correct solution of (20) will never overshoot equilibrium [12]. However, obtaining this solution requires solving a non-linear system of equations by an iterative scheme such as the Newton–Raphson method.

Asymptotic Integration

A popular approach towards solving stiff systems in the form (19) has been the use of exponential integrators [13, 14]. The basic idea is that one gets rid of stability restrictions on the time step by approximating the stiff component of the solution as an exponential function. Recently, exponential methods tailored for relaxation systems have been proposed [12]. The first order method, referred to as ASY1, is given by

$$q^{n+1}_i = q^*_i + (q^{\mathrm{eq}}_i - q^*_i) \left[1 - \exp\left(-\frac{\Delta t}{\tau_i}\right) \right], \tag{21}$$

where $\boldsymbol{q}^{\mathrm{eq}}$ is the equilibrium state and

$$\tau_i = \frac{q^{\mathrm{eq}}_i - q^*_i}{s_i(\boldsymbol{q}^*)}. \tag{22}$$

The scheme (21)–(22) is unconditionally stable by construction, but it requires knowledge of the equilibrium state.

When mass is moved from one phase to the other, total mass and energy are always conserved, as seen from Eq. (4), and by adding Eqs. (1) and (2). Thus, to calculate the equilibrium state for the mass transfer process, we need to find the pressure p and temperature T as functions of the mixture density ρ and internal energy $E_{\mathrm{int}} = \alpha_{\mathrm{g}} \rho_{\mathrm{g}} e_{\mathrm{g}} + \alpha_\ell \rho_\ell e_\ell$, such that $\mu_{\mathrm{g}} = \mu_\ell$. This corresponds to finding the boiling point for the given mixture density and internal energy.

In order to accomplish this, two nested Newton–Raphson algorithms were used. The algorithm may be briefly summarized as follows:

1. Guess a pressure p_{boil}.

2. Find boiling point $T_{\mathrm{boil}}(p_{\mathrm{boil}})$ by solving $\mu_{\mathrm{g}} = \mu_\ell$ using Eq. (10) and the Newton–Raphson method.

3. Solve

$$\rho_g(\rho - \rho_\ell)e_g + \rho_\ell(\rho_g - \rho)e_\ell - (\rho_g - \rho_\ell)E_{int} = 0$$

evaluated at $(p, T) = (p_{boil}, T_{boil})$ and update the pressure using one step of a Newton–Raphson method.

4. Go to step 2 until desired accuracy is reached.

For our particular model, both the Backward Euler and ASY1 schemes require solving an iterative problem in each computational step. The relative stability and efficiency of these two schemes thus hinge on the stability and efficiency obtainable in their respective iterative schemes.

4   RESULTS

In this section, we will present results for depressurisation of a pipe with pure CO_2. The pipe has a length of $L = 80$ m, and is initially filled with liquid CO_2 at a pressure of $p = 60$ bar in the left part ($x \leq 50$ m) and gas at 10 bar in the right part ($x > 50$ m). The parameters used for the stiffened gas equation of state are shown in Table 1. The CFL number used was $C = 0.5$, while the initial volume fraction was $\delta = 0.01$. This case was also used in Ref. [5], but in the present paper we focus more on the results of different numerical methods.
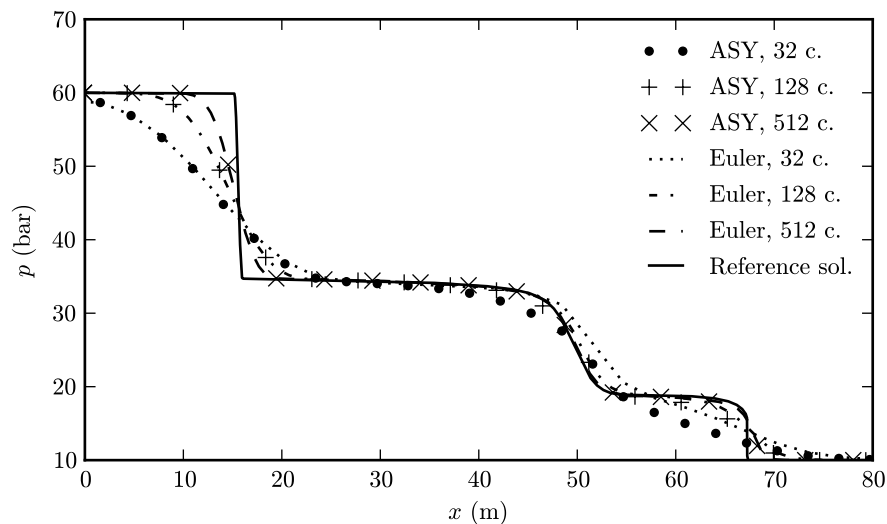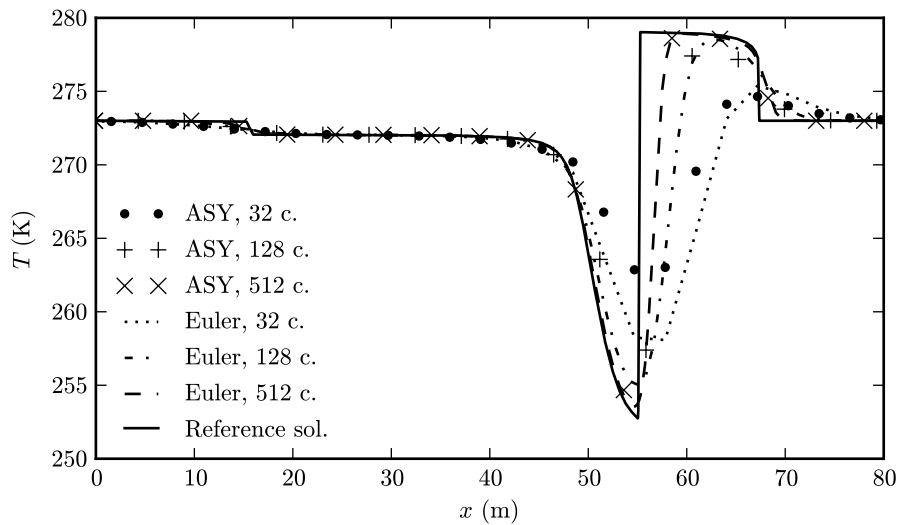

Figure 2: Pressure at time $t = 0.08$ s

As time progresses, pressure waves will propagate to the left and right through the liquid and gas, respectively. Between these two pressure fronts, phase transfer in the form of evaporation and condensation will take place. Figure 2 shows the pressure after time $t = 0.08$ s, comparing the solutions using the ASY1 method and the Backward Euler method to a reference solution. The reference solution was obtained using a second order method and a very fine grid. In this reference solution, to the left of the front at $x \approx 16$ m, there is pure liquid, while there is pure gas to the right of $x \approx 55$ m.

From Figure 2, we see that the two methods have very similar results with equal grid size. In the right part of the plot, we see that ASY1 is slightly more diffusive than the Backward Euler method with 32 grid cells. This difference between the two methods is perhaps even clearer in Figure 3, which shows the temperature for the same case. The temperature dip around $x \approx 55$ m is seen to be much clearer with the Backward Euler method than the ASY1 method, especially with the coarsest grids.

Table 2 shows the computational time spent for a range of different grid sizes, to give an impression of how the computational cost for the two methods are related. As seen in this table, the time spent is rather similar for the same grid size, although the ASY1 scheme seems to have slightly better performance. It can be noted that the computational cost for the ASY1 method comes from calculating the equilibrium state, while the cost in the Backward Euler method is due to a Newton–Raphson iteration in the numeric scheme (20) itself. The cost for these two approaches may vary with different formulations of the source term than the one we have presented here, as

Figure 3: Temperature at time $t = 0.08$ s

it in some cases is possible to calculate the equilibrium state relatively cheap, in which case the ASY1 scheme would be expected to outperform the Backward Euler scheme. Since the methods produce similar results at similar computational cost, there does not seem to be any reasons to prefer one in front of the other for the case we have presented here.

Table 1: Stiffened gas parameters used in the simulation

Phase	γ (–)	p_∞ (Pa)	c_v (J/kg K)	e_* (J/kg)	s_0 (J/kg K)	ρ_0 (kg/m^3)	T_0 (K)
Gas	1.06	$8.86 \cdot 10^5$	$2.41 \cdot 10^3$	$-3.01 \cdot 10^5$	$1.78 \cdot 10^3$	135	283.13
Liquid	1.23	$1.32 \cdot 10^8$	$2.44 \cdot 10^3$	$-6.23 \cdot 10^5$	$1.09 \cdot 10^3$	861	283.13

Table 2: Computational time (in seconds) on a single Intel Core2 at 2.8 GHz for a range of different grid sizes

Grid size	ASY1	Euler
512	6.23	7.15
1024	24.45	27.78
2048	99.26	110.71
4096	389.56	442.50

A final point we would like to make, is that our method is able to handle regions with volume fractions α_k of exactly zero. For other numerical methods found in the literature, it is often necessary to have non-zero volume fractions to avoid numerical instabilities [15, 16]. Our approach has not shown to exhibit any such instabilities.

5 CONCLUSION

We have presented a two-phase flow model with phase transfer modelled using a relaxation term based on statistical rate theory. This model was solved using a first-order Godunov splitting scheme, making it possible to solve the hyperbolic equation system and the phase transfer model separately. We have shown results for two different approaches to solving the phase transfer numerically, one based on the Backward Euler method and one on the time-asymptotic ASY1 scheme. The ASY1 scheme has the advantage of being explicit if only the equilibrium state is known. However, with the particular model we have considered, calculating the equilibrium state is done iteratively, which gives the ASY1 method similar performance to the Backward Euler method when it comes to accuracy and computational cost. In future work, it could be investigated whether a second-order splitting scheme is benifical when solving models similar to the one presented here.

ACKNOWLEDGEMENT

REFERENCES

[1] T. Flåtten, A. Morin, and S. T. Munkejord. Wave propagation in multicomponent flow models. *SIAM Journal on Applied Mathematics*, **70**(8):2861–2882, Sep 2010.

[2] C. A. Ward, R. D. Findlay, and M. Rizk. Statistical rate theory of interfacial transport. I. Theoretical development. *The Journal of Chemical Physics*, **76**(11):5599–5605, 1982.

[3] C. A. Ward and G. Fang. Expression for predicting liquid evaporation flux: Statistical rate theory approach. *Phys. Rev. E*, **59**(1):429–440, Jan 1999.

[4] Y.-P. Pao. Application of kinetic theory to the problem of evaporation and condensation. *Physics of Fluids*, **14**(2):306–312, 1971.

[5] H. Lund and P. Aursand. Two-phase flow of CO_2 with phase transfer. *Energy Procedia*. Accepted for publication, preprint available at `http://folk.ntnu.no/halvorlu`.

[6] R. Menikoff and B. J. Plohr. The Riemann problem for fluid flow of real materials. *Rev. Mod. Phys.*, **61**:75–130, 1989.

[7] R. J. LeVeque. *Finite Volume Methods for Hyperbolic Problems*. Cambridge University Press, 2002.

[8] E. F. Toro. Multi-stage predictor-corrector fluxes for hyperbolic equations. Technical Report NI03037-NPA, Isaac Newton Institute for Mathematical Sciences, University of Cambridge, UK, 17th June 2003.

[9] E. F. Toro. *Riemann solvers and numerical methods for fluid dynamics*. Springer-Verlag, Berlin, second edition edition, 1999. ISBN 3-540-65966-8.

[10] V. A. Titarev and E. F. Toro. MUSTA schemes for multi-dimensional hyperbolic systems: analysis and improvements. *International Journal for Numerical Methods in Fluids*, **49**:117–147, 2005.

[11] S. T. Munkejord, S. Evje, and T. Flåtten. The multi-stage centred-scheme approach applied to a drift-flux two-phase flow model. *International Journal for Numerical Methods in Fluids*, **52**(6):679–705, October 2006.

[12] P. Aursand, S. Evje, T. Flåtten, K. E. T. Giljarhus, and S. T. Munkejord. An exponential time-differencing method for monotonic relaxation systems. *Preprint*, 2010. Available at `http://www.math.ntnu.no/conservation/2011/008.pdf`.

[13] M. Hochbruck, C. Lubich, and H. Selhofer. Exponential integrators for large systems of differential equations. *SIAM J. Sci. Comput.*, **19**:1552–1574, 1998.

[14] S. M. Cox and P. P. Matthews. Exponential time differencing for stiff systems. *J. Comput. Phys.*, **176**:430–455, 2002.

[15] S. T. Munkejord, S. Evje, and T. Flåtten. A MUSTA scheme for a nonconservative two-fluid model. *SIAM J. Sci. Comput.*, **31**(4):2587–2622, 2009.

[16] C.-H. Chang and M.-S. Liou. A robust and accurate approach to computing compressible multiphase flow: Stratified flow model and AUSM+-up scheme. *Journal of Computational Physics*, **225**(1):840–873, 2007.

The remainder of this page was intentionally left blank.